Constraining near-fault ground motion simulations : the potential of observations of displaced grave slabs

Mathieu Causse, Christos Lachanas, Dimitrios Vamvatsikos, Laurent Baillet

18TH WORLD CONFERENCE ON EARTHQUAKE ENGINEERING
WCEE2024
MILAN

MILAN, ITALY
30TH JUNE - 5TH JULY 2024

www.wcee2024.it

CONSTRAINING NEAR-FAULT GROUND MOTION SIMULATIONS: THE POTENTIAL OF OBSERVATIONS OF DISPLACED GRAVE SLABS

M. Causse[1], C.G. Lachanas[2], D. Vamvatsikos[2] & L. Baillet[1]

[1] ISTerre, Univ. Grenoble Alpes, Univ. Savoie Mont Blanc, CNRS, IRD, Univ. Gustave Eiffel, 38000 Grenoble, France ddress

[2] School of Civil Engineering, National Technical University of Athens, Greece

Abstract: *The number of seismological observations available in the vicinity of faults is still too limited to fully catch the complexity of strong motion and properly calibrate Ground Motion Models (GMMs). This problem is exacerbated in areas of moderate seismicity, where earthquakes often occur on unknown faults and are only exceptionally recorded in damage areas. Physics-based simulation methods are a very promising approach but they require a very good understanding of the physical processes controlling the strong motion (variability of the rupture process, radiation of high frequency seismic energy, effects of shallow geological structures, etc.), which also requires more observations. Here we propose an approach to constrain near-fault ground motion predictions based on measures of grave slab sliding displacements, e.g., as observed during the Le Teil earthquake in 2019 (Mw 4.9, France) and in Petrinja in 2020 (Mw 6.4, Croatia). In a Bayesian framework, the approach combines a priori information on the ground motion distribution obtained using physics-based simulations and a likelihood function representing the probability of the observed slab displacement for a given ground motion intensity measure, to produce a posterior distribution of ground-motions.*

1 Introduction

In view of the small number of near-fault accelerograms, especially in intraplate tectonic settings, the probability to record an earthquake in the vicinity of a fault remains very small. This limits our ability to predict strong ground motion for potential future events. To approximate seismic intensity, field reports of earthquake damage have long reported observations of displaced objects, such as toppling of tombstones and other objects in graveyards, mainly in Japan (e.g. Ikegami et al. 1947; Abe 1974; Omote et al. 1975). The modeling of the toppling of fragile geological structures—such as "precarious rocks", i.e., boulders in unstable equilibrium, or rock columns—have been widely used to establish the level of ground motion exceeded or not at a given site, and to refine probabilistic estimates of seismic hazard for long return periods (e.g. Brune & Whitney 1992; Ambraseys & Psycharis 2013; Rood et al. 2020). In addition, observations of rigid sliding blocks also bring information on the ground motion level. For instance, reported displacements of objects in buildings such as cupboards or stoves during the 1969 Banja Luka earthquake (Bosnia) were used to estimate ground acceleration, based on a posteriori measures of the friction coefficients.

The sliding of objects can however be complex to model as it can sometimes be combined with toppling (e.g. Gazetas et al. 2012; Garini et al. 2017).

Herein we propose an approach to constrain near-fault ground motion simulations based on observations of grave slab displacements, e.g., as observed during the Le Teil earthquake in 2019 (Mw 4.9, France) and in Petrinja in 2020 (Mw 6.4, Croatia). The potential of the method lies in: (1) the multiplicity of potential observations—as an example, France has 40,000 cemeteries, mainly in urban areas, representing an exceptional coverage; (2) the relative simplicity of modeling the targeted structures that can be found in many countries including France, Italy, Greece and Iran, i.e. slabs lying freely on their bases, without toppling possibility; (3) the very low cost of in-situ measurement of observed funeral slab displacements in the epicentral area following an earthquake. The approach is illustrated using data of ground motion simulations and graveyards displacements provided for the 2019 Mw 4.9 Le Teil earthquake (Rhône river valley, southeast of France) by Causse et al. (2021). Moreover, the on-field sliding observations are employed within a generic approach for the Bayesian update of the ground motion intensity as proposed by Vamvatsikos and Lachanas (2022).

2 A Bayesian framework to constrain the IM distribution

Let's imagine we are on a post-seismic mission. Among the post-seismic observations, a grave slab has experienced a residual relative displacement equal to d_{obs} at a site S. The earthquake rupture has characteristics C including magnitude, fault mechanism, slip distribution, rupture velocity, etc. We are interested in estimating at the site $P(IM = x|d = d_{\text{obs},}, S, C)$, where IM represents a ground motion intensity measure. For practical reasons, we consider in the following discrete probabilities rather than probability densities [Vamvatsikos and Lachanas (2022)]. In other words, the later expression is meant to be determined by discretizing *x* in bins. As such, it represents the probability that the IM lies in a small interval around *x*, given the observed grave slab displacement and knowing site and rupture characteristics *S* and *C.*

By modeling the residual displacement of a grave slab (for instance by means of a Coulomb friction model) for a given IM, and knowing *S* and *C*, one can actually obtain $P(d = d_{\text{obs}}|IM = x, S, C)$. This is the inversed conditional quantity of what we are actually looking for. The two expressions however can be simply related if we apply the Bayes theorem:

$$P\big(IM = x\big|d = d_{\text{obs},}, S, C\big) = \frac{P(d = d_{\text{obs}}|IM = x, S, C)\ P(IM = x|S, C)}{P(d = d_{\text{obs}}|S, R)} \qquad (1)$$

The term $P(IM = x|S, C)$ represents the *a priori* information on the IM distribution. Depending on the level of information on the site and source characteristics, any approach such as Ground Motion Models or physics-based ground motion predictions can be used. Equation (1) provides the posterior distribution of IM, i.e. the distribution updated to include information provided by the observed displaced slab. The term $P(d = d_{\text{obs}}|IM = x, S, C)$ requires probabilistic modeling of the grave slab sliding. The sliding response of rigid bodies has been extensively studied for earthquake engineering applications [e.g., Newmark (1965); Choi and Tung (2002); Konstantinidis and Nikfar (2015)]. Vamvatsikos and Lachanas (2022) have proposed the direct usage of the structural fragility for exceeding a given d_{obs} value $P(d > d_{\text{obs}}|IM = x, S, C)$ in Eq. (1); this implies that the IM is a sufficient predictor of *d* (Luco and Cornell 2007), which allows dropping the conditioning on *S* and *R*. For sliding, such a relatively sufficient IM seems to be the PGV (Lachanas et al. 2024), which will be employed henceforth.

Then, if we need the probability of equaling, $P(d = d_{\text{obs}}|IM = x)$, then we can employ the fragility $P(d > d_{\text{obs}}|IM = x)$ and take its difference between the bounds of a small range around d_{obs}, thus working with the probability of being within this range instead of exceeding d_{obs}. In

principle, the length of the interval around d_{obs} should depend on the level of uncertainty on d_{obs}, including both measurement and modeling errors.

Finally, $P(d = d_{\text{obs}} | S, C)$ is the probability that the slab displacement equals d_{obs}, given that an event with characteristics *S* and *C* has occurred. It can be easily treated by the total probability theorem:

$$P(d = \text{d}_{\text{obs},}, S, C) = \int_0^\infty P(d = \text{d}_{\text{obs}} | IM = x') \; P(IM = x | S, C) \, dx' \qquad (2)$$

In most cases there will be several observations with a certain dispersion of the measured gave slab displacements, due for instance to variability of the friction properties or orientation of the slabs, or small-scale spatial variability of the ground motion in the visited graveyard. In practice, one can then consider bins of *d* values and the proportion r_i of observations within each bin $[d_{\text{inf},i}, d_{\text{sup},i}]$. Following Vamvatsikos & Lachanas (2022), we can apply a logic tree approach:

$$P\big(IM = x \big| d = d_{\text{obs},}, S, R\big) = \sum_i r_i \; P\big(IM = x \big| d \in [d_{\text{inf},i}\,, d_{\text{sup},i}\,], S, R\big) \qquad (3)$$

where the probability terms in the sum are computed using Eq. 2.

A simplified approach consists of considering the proportion r_1 of observed slab displacements above a given threshold d_{lim} rather than bins of *d* values. In this case, Eq. 3 can replaced by:

$$P(IM = x | r_1, S, R) = r_1 \; P(IM = x | d > d_{lim}, S, R) + (1 - r_1) P(IM = x | d \leq d_{lim}, S, R) \quad (4)$$

Again, the probability terms in the sum can be estimated using Eq. 2 by replacing $P(d = \text{d}_{\text{obs}} | IM = x)$ by $P(d > d_{\text{lim}} | IM = x)$ or $P(d \leq d_{\text{lim}} | IM = x)$.

3 Application to the 2019 M_W 4.9 Le Teil earthquake

On November 11, 2019, a Mw 4.9 earthquake occurred in the south east of France within the lower Rhône river valley, a moderate seismicity area. The unexpected level of damage for this magnitude (epicentral intensity VIII) indicates an intense ground shaking. Unfortunately, strong motion was not recorded by accelerometric sensors in the damage area, near the fault. This event is characterized by a reverse-fault mechanism, a rupture area of about 4 km by 1.5 km, a hypocenter at 1 km and evidence of surface rupture (Ritz et al. 2020). Such a shallow rupture, which is exceptional for a moderate-sized event, explains the locally-high damage level.

To estimate the level of near-fault ground motion, Causse et al. (2021) performed 1D numerical ground motion simulations considering a set of kinematic rupture models (1000 rupture realizations). Given the large uncertainty in the rupture kinematics, they obtained uncertainty levels on the simulated IM of a factor of 2 to 4. In addition, they reported observations of grave slab displacements in a graveyard located a few hundreds of meters away from the fault, with an average displacement of about 5 cm. By modeling the sliding response of a grave slab for each of the 1000 ground motions simulated at the graveyard site, they showed that the observations support, to a 1st order, the average value of the numerically simulated IMs. Causse et al. (2021) modeled a grave slab as a mass particle with three degrees of freedom. The particle, subjected to gravitational force, is in frictional contact with the EW-NS plane, which is animated by the three-dimensional ground motion. A standard Coulomb friction model was assumed. Since each slab is adjacent to a headstone, their motion is not possible in all directions. During the motion, a perfectly inelastic collision was then imposed on the slab, which cannot penetrate the headstone. The particle motion was solved using a forward incremental Lagrange multiplier method (Baillet et al. 2003).

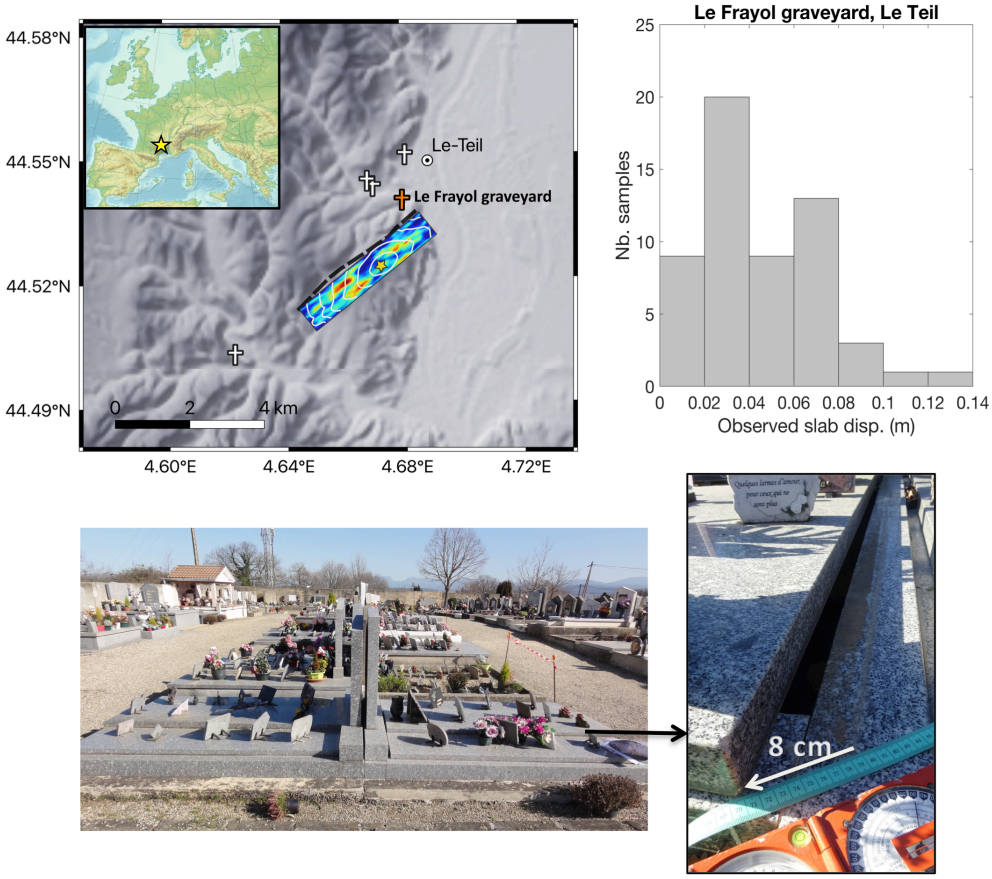

Figure 1: (top left) location of the Le Teil 2019 earthquake. The colored rectangle shows one realization of rupture kinematics. The orange cross indicates the location of the Frayol graveyard. The distribution of the observed displacement values is shown on the top right. The bottom figures show one example of displaced grave slab with a typical configuration (slab resting on its base with a headstone on one end).

Here we use the set of numerical ground-motion simulations and the database of observed and modeled grave slab displacements of Causse et al. (2021) to illustrate the Bayesian method described in Section 2. The set of numerical ground-motion simulations at the graveyard provides a sample of 1000 PGV values used as *a priori* information. We then use Eq. 3 to compute the posterior probability density function (PDF) of PGV. Fig. 2 shows both the prior and posterior PDF considering static friction coefficients of 0.2 and 0.4. The information from the slab displacements results in a significant increase of the median PGV value, from 20 cm/s to 27 cm/s for μ=0.2 and 47 cm/s for μ=0.4 (Fig. 2, left). Fig. 2 (right) also compares the posterior PDF obtained considering a model in which the slab is adjacent to a headstone (as in Fig. 2, left), preventing it from moving in one direction, with a model in which the slab rests freely on its base (i.e. allowed to move in all directions). The results indicate that the assumption of a freely resting slab tends to slightly overestimate the median PGV. This is because the energy accumulated by the headstone, as the inertial forces applied to the slab point towards the headstone, tends to increase the slab displacement in the opposite direction (Fig. 2, right). To obtain robust PGV estimates, the friction coefficient is however the main parameter to constrain.

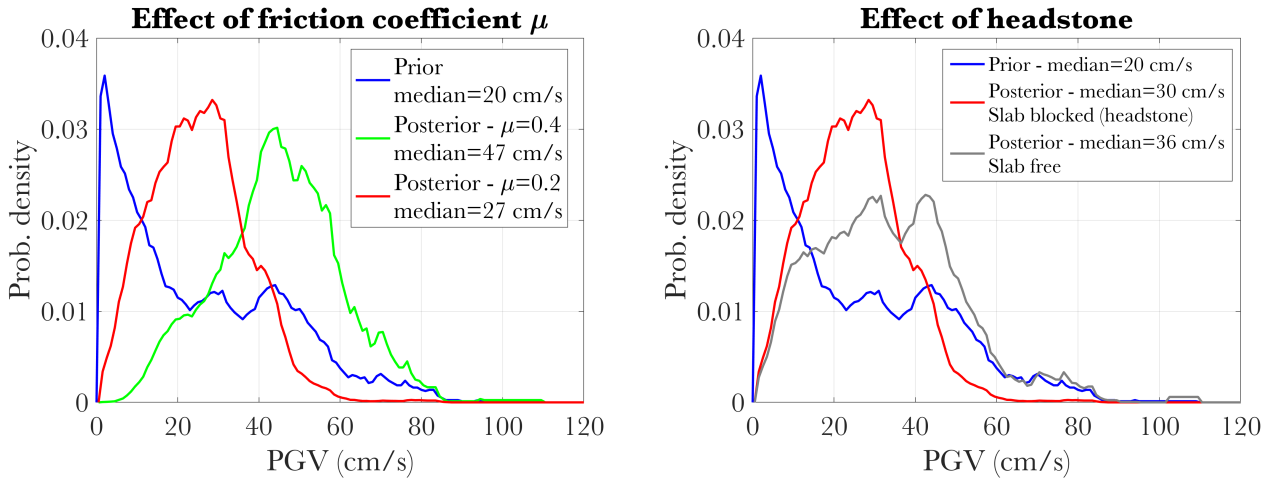

Figure 2: Prior and posterior PDF of PGV estimated for the Le Teil earthquake at the Frayol graveyard using Eq. 3. The left figure illustrates the impact of the friction coefficient, while the right figure shows the impact of different assumptions to model the slab displacement (slab freely resting on its base or constrained by an adjacent headstone).

Finally, Figure 3 compares the posterior PDF obtained using Eq. (3) and Eq. (4). Obviously, the results from Eq. (4) depend on the chosen threshold value d_{res}. In this particular example, choosing a very small value of d_{lim} provides the most informative result. In this case r_1 is close to 1, and since sliding is essentially observed for PGV values above ~10 cm/s, the peak observed at small PGV values (<~10 cm/s) in the prior PGV distribution is shifted to higher values. For d_{lim} values above 5 cm, the prior PDF is almost not modified, so that the there is no information brought by the observations.

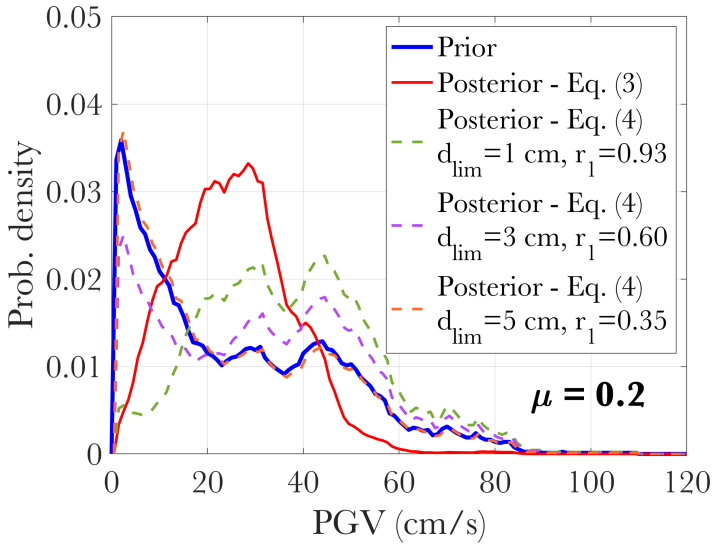

Figure 3: Comparison between posterior PDF of PGV obtained using Eq. (3) and (4). Eq. (4) is applied considering various values of the threshold slab displacement d_{lim}.

4 Towards a simplified approach

The method presented above uses a set of numerical ground motion predictions to define the a priori PDF of IM. The simulated ground motion is next used to model the slab motions. The numerical simulations by Causse et al. (2021) are based on several information about the rupture (C) and site (S) that cannot be quickly available, including a “local” velocity model obtained from

seismic noise analysis, kinematic rupture models consistent with geodetic and regional seismological observations. For a rapid estimation of the IM distribution after a seismic event (for instance for application to Shakemaps) one can easily replace the numerical simulations with a GMM. One can also imagine to simplify Eq. 4 by replacing the term $P(IM = x|d > d_{lim}, S, C)$ by a term $P(IM = x|d > d_{lim})$, i.e. predefined fragility curves computed from a database of strong motion data without constraints on S and C. For our example, the proposed closed-form equations for sliding fragilities as proposed by Lachanas et al. (2024) are employed. These equations have been constructed after running incremental dynamic analysis (IDA, Vamvatsikos and Cornell 2002) under a suite of ordinary (no-pulse-like, no-long-duration) ground motions to sliding rigid blocks and then applying a curve fitting procedure to the 16/50/84% IDA quantiles. A Newmark planar sliding block model (Newmark 1965) with static Coulomb friction was used as described by Tsarpalis et al (2022) to capture the two-way sliding response. The proposed expressions for the fitted IDA quantiles in companion with a proper statistical distribution can be employed for the direct construction of the corresponding fragility curve for any given level of intensity or response. They can be used for the rapid seismic design and/or assessment of sliding rigid blocks in a similar way like the recently proposed closed-form equations for rocking blocks (Kazantzi et al. 2021; Kazantzi et al. 2022).

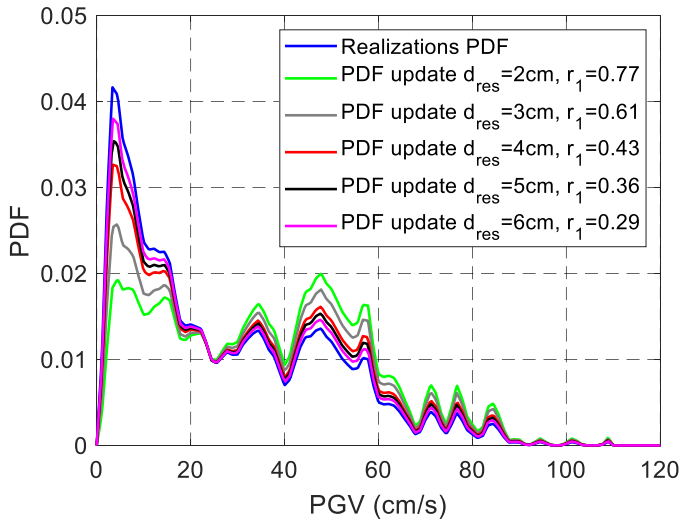

Figure 4: Comparison between posterior PDF of PGV obtained using Eq. (4) for the simplified approach of using the fragility curves of exceeding specific d_{lim} values and the corresponding percentage of exceeding the same values from the on-field observations.

5 Conclusion

We proposed an approach to constrain near-fault ground motion simulations based on observations of grave slab displacements. The principle is to employ on-field sliding observations within a generic approach for the Bayesian update of the simulated ground motion IM as proposed by Vamvatsikos and Lachanas (2022). The approach is illustrated using data of ground motion simulations and graveyards displacements provided for the 2019 Mw 4.9 Le Teil earthquake (Causse et al. 2021). The proposed approach may provide robust PDF estimates of the PGV provided that the friction coefficient is well constrained, for instance from in-situ measurements. We also tested a simplified approach, in which generic closed-form equations for sliding fragilities are employed (Lachanas et al. 2024), that may be useful for rapid estimation of ground motion IM following an earthquake.

6 References

Ambraseys, N., Psycharis, I.N.: Assessment of the long term seismicity of Athens from two classical columns. Bulletin of Earthquake Engineering 10(6), 1635-1666 (2012).

Baillet, L., V. Linck, S. D'Errico, B. Laulagnet and Y. Berthier. Finite element simulation of dynamic instabilities in frictional sliding contact. In STLE/ASME 2003 International Joint Tribology Conference (pp. 25–30). (American Society of Mechanical Engineers Digital Collection, 2003)

Brune, J.N., Whitney, J.W.: Precariously balanced rocks with rock Varnish Paleoindicators of maximum ground acceleration. Seismological Research Letters 63(1), 21 (1992).

Causse, M., Cornou, C., Maufroy, E., Grasso, J. R., Baillet, L., & El Haber, E. (2021). Exceptional ground motion during the shallow Mw 4.9 2019 Le Teil earthquake, France. Communications Earth & Environment, 2(1), 14.

Choi B., Tung C.C.D. (2002). Estimating sliding displacement of an unanchored body subjected to earthquake, Earthquake Spectra, 18(4): 601-613.

Garini, E., Gazetas, G., & Anastasopoulos, I. (2017). Evidence of significant forward rupture directivity aggravated by soil response in an Mw6 earthquake and the effects on monuments. Earthquake Engineering & Structural Dynamics, 46(13), 2103-2120.

Gazetas, G., Garini, E., Berrill, J. B., & Apostolou, M. (2012). Sliding and overturning potential of Christchurch 2011 earthquake records. Earthquake engineering & structural dynamics, 41(14), 1921-1944.

Ikegami, R., Kishinoue, F.: A study on the overturning of rectangular columns in the case of the Nankai Earthquake on December 21, 1946. Bulletin of the Earthquake Research In-stitute, University of Tokyo, 25, 49–55 (1947).

Kazantzi A.K., Lachanas C.G., Vamvatsikos D. (2021). Seismic response distribution expressions for on-ground rigid rocking blocks under ordinary ground motions, Earthquake Engineering and Structural Dynamics, 50(12): 3311-3331.

Kazantzi A.K., Lachanas C.G., Vamvatsikos D. (2022) Seismic response distribution expressions for rocking building contents under ordinary ground motions, Bulletin of Earthquake Engineering, 20: 6659-6682.

Konstantinidis D., Nikfar F. (2015). Seismic response of sliding equipment and contents in base-isolated buildings subjected to broadband ground motions, Earthquake Engineering & Structural Dynamics, 44(6): 865-887

Kottke, A., Whittaker, A.C., Page, W.D., Stafford, P.J.: Earthquake hazard uncertainties improved using precariously balanced rocks. AGU Advances 1(4), e2020AV000182 (2020).

Lachanas C.G., Vamvatsikos D., Causse M., Kotha S.R. (2024). The effect of ground motion characteristics on the sliding of rigid bodies and the role of intensity measures. Proceedings of the 18th World Conference of Earthquake Engineering, Milan, Italy.

Luco, N., & Cornell, C. A. (2007). Structure-specific scalar intensity measures for near-source and ordinary earthquake ground motions. Earthquake Spectra, 23(2), 357-392.

Newmark N.M. (1965). Effects of Earthquakes on Dams and Embankments, Géotechnique, 15(12): 139-160.

Omote, S., Miyake, A., and Narahashi, H.: Maximum ground acceleration in the epicentral area—Field studies on the occasion of the Ohita Earthquake, Japan, of April 21, 1975. Bul-letin of the International Institute of Seismology and Earthquake Engineering 15, 67–82 (1977).

Ritz, J. F., Baize, S., Ferry, M., Larroque, C., Audin, L., Delouis, B., & Mathot, E. (2020). Surface rupture and shallow fault reactivation during the 2019 Mw 4.9 Le Teil earthquake, France. Communications Earth & Environment, 1(1), 10.

Rood, A.H., Rood, D.H., Stirling, M.W., Madugo, C.M., Abrahamson, N.A., Wilcken, K.M., Gonzalez, T.,

Tsarpalis D., Vamvatsikos D., Vayas I. (2022). Seismic assessment approaches for mass-dominant sliding contents: The case of storage racks, Earthquake Engineering and Structural Dynamics, 51(4): 812–831.

Vamvatsikos, D. & Lachanas, C.G. Tomb Raiders of the Lost Accelerogram: A Fresh Look on a Stale Problem. In : European Conference on Earthquake Engineering and Seismology. Cham : Springer International Publishing, 2022. p. 62-73.

Vamvatsikos D., Cornell C.A. (2002). Incremental dynamic analysis. Earthquake Engineering and Structural Dynamics, 31(3): 491-514.